TUDelft

Delft University of Technology

Statistical Analysis of the Stability of Rock Armoured Slopes

van Gent, Marcel; de Almeida Sousa, Ermano; Hofland, Bas

Important note
To cite this publication, please use the final published version (if applicable).
Please check the document version above.

STATISTICAL ANALYSIS OF THE STABILITY OF ROCK ARMOURED SLOPES

MARCEL R.A. VAN GENT [1], ERMANO DE ALMEIDA [1,2], BAS HOFLAND [1,2]

[1] *Deltares, The Netherlands, Marcel.vanGent@deltares.nl*

[2] *Delft University of Technology, The Netherlands, E.deAlmeida@tudelft.nl; B.Hofland@tudelft.nl*

ABSTRACT

Physical model tests were performed in a wave flume at Deltares with rock armoured slopes. A shallow foreshore was present. At deep water the same wave conditions were used but, by applying different water levels, the wave loading on the rock armoured slopes increased considerably with increasing water levels. This allows the assessment of effects of sea level rise. Damage has been measured by using Digital Stereo Photography (DSP) which provides information on each individual stone that has been displaced. Two test series have been performed five times. This allows for a statistical analysis of the damage to rock armoured slopes. The statistical analysis demonstrates the need to take the spreading around a mean damage into account in the design of rock armoured slopes. This is important in addition to characterising the damage itself by erosion areas and erosion depths. The relation between damage parameters such as erosion area and erosion depth has been obtained from the tests. Besides tests with a straight slope also tests with a berm in the seaward slopes have been performed. A method to take the so-called length effect into account has been proposed to extrapolate results from physical model tests to real structures. Use is made of standard deviations based on the presented model tests.

KEYWORDS: Stability; Erosion; Rock slopes; Sea level rise; Repetition tests; Berm; Wave flume; Length effect.

1   INTRODUCTION

Due to sea level rise the wave loading on sea defences can become more severe. This is especially the case for sea defences in shallow water. Depth-limited waves at the toe of structures become larger for increasing water levels, for equal wave conditions at deep water. Thus, not only the direct influence of increasing water levels that cause that the sea defence is more vulnerable to wave overtopping, also the wave loading is affected by the sea level rise. The increasing wave loading on structures affects wave overtopping but also the stability of the armour. Here, effects of increasing water levels on the stability of rock armoured slopes have been studied for conditions that are equal at deep water but more severe at the toe of the structure.

The stability of rock armoured slopes has been studied by performing physical model tests in a wave flume. Tests with rock armoured slopes were performed with straight slopes and with a berm in the seaward slope. Damage was measured using Digital Stereo Photography (DSP) and characterised by using various damage parameters. Two series of tests (those without a berm) were performed five times which allows for a statistical analysis of the results by taking into account the spreading in the test results. Besides the spreading in test results in the wave flume (see also Melby and Kobayashi, 1998), also in reality spreading of damage occurs. For longer structures, the risk increases that at a particular location along this structure the damage exceeds a specified maximum allowable damage. Guidance to take this length effect into account in the design of rock armoured slopes is provided.

2   PHYSICAL MODEL TESTS

Physical model tests have been performed in the Scheldt Flume of Deltares, Delft (width 1 m, height 1.2 m, length 110 m of which 55 m were used in this study). The wave board is equipped with Active Reflection Compensation (ARC). This means that the motion of the wave board compensates for the waves reflected by the structure preventing them to re-reflect back into the model. The wave board is equipped with second order wave steering. This means that second order effects of the first higher and lower harmonics are taken into account in the wave board motion. This wave generation system ensures that the generated waves resemble waves that occur in nature.

Figure 1 shows the cross-section of the test set-up in the flume. A horizontal shallow foreshore was present in front of the structure. The transition slope from deep water to this shallow horizontal foreshore was close to 1:15. Five structure configurations were tested. One with a straight slope (see Figure 2) and four with a berm (see Figure 3); a narrow (0.08m, *i.e.* a width of 5 stone diameters: 5 D_{n50}) and a wide berm (0.16m, *i.e.* 10 D_{n50}), each at two different levels. The tested structures consisted of an armour layer of rock with a D_{n50} of 0.0163m, a grading of $D_{n85} / D_{n15} = 1.25$, density of ρ_s=2710 kg/m^3 and a layer thickness of two diameters, a filter layer of rock with D_{n50} of 0.0094m, and a layer thickness of two diameters, on a 1:3 slope with an impermeable core. The crest level was fixed at 0.296m above the toe of the structure (non-overtopped).
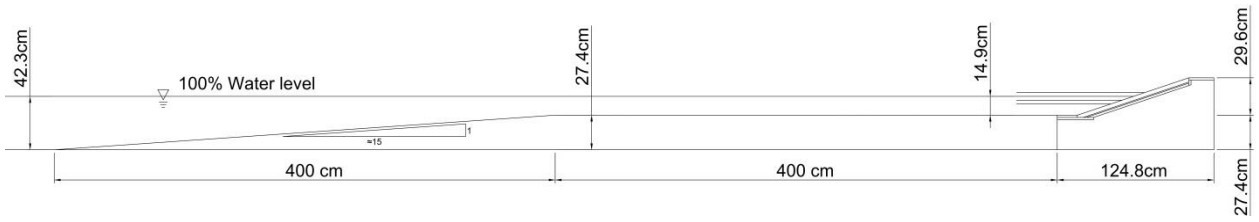
Figure 1. Foreshore and structure geometry in the wave flume.
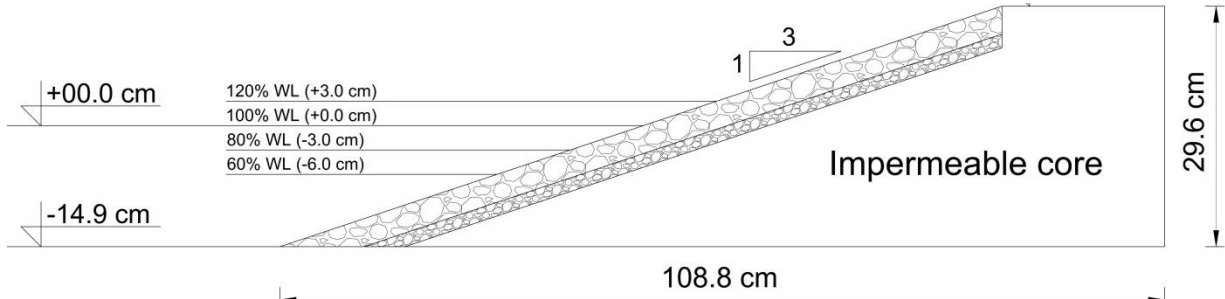

Figure 2. Structure geometry with a straight slope.
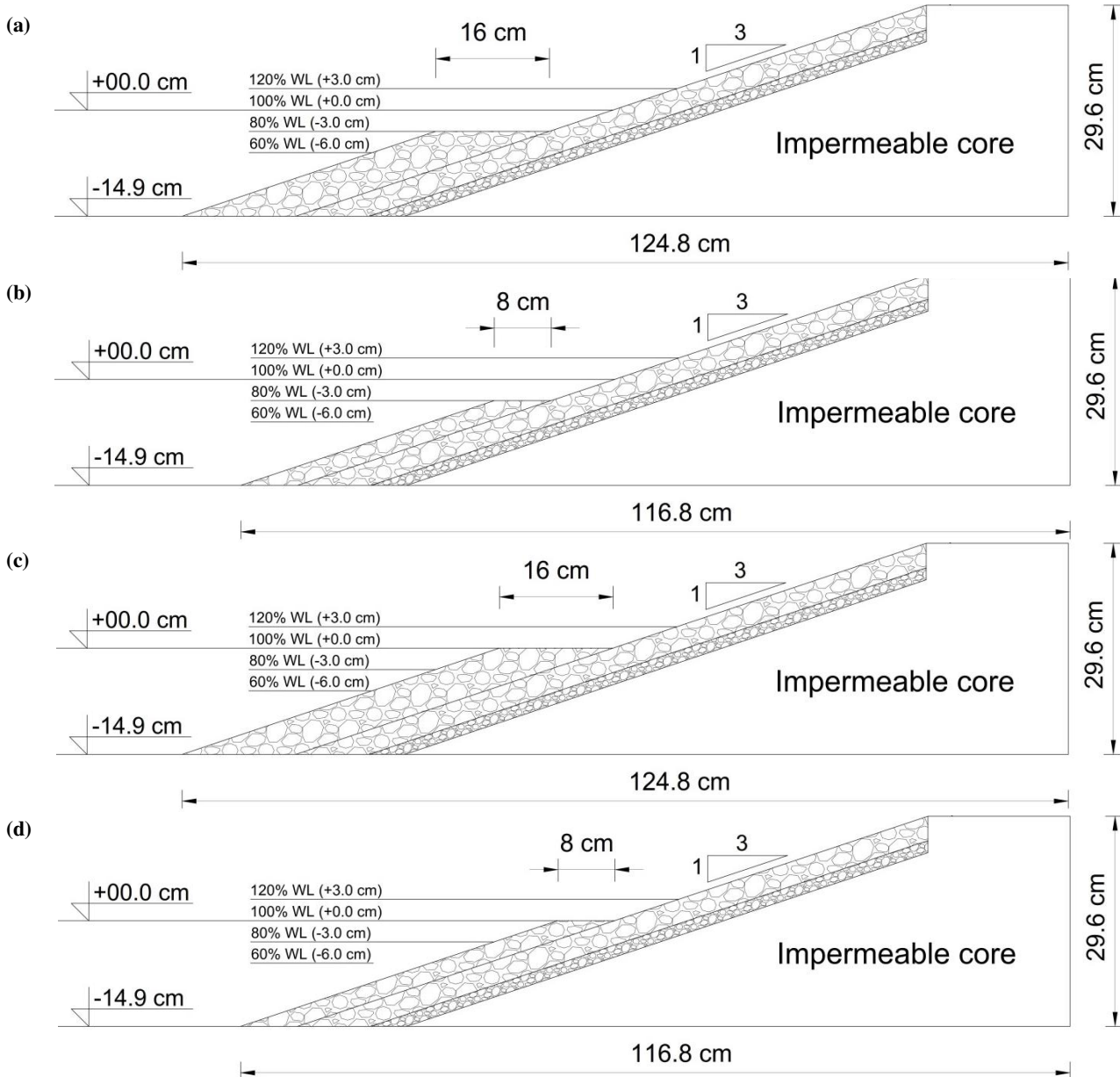

Figure 3. Structure geometries with berms (*a*: Wide berm at a level of "80% of the 100% WL"; *b*: Narrow berm at "80% of the 100% WL"; *c*: Wide berm at a level of the "100% WL"; *d*: Narrow berm at the "100% WL").

The deep water conditions were always the same, namely a spectral significant wave height of H_{m0}=0.088m and a peak wave period of T_p=1.27s (wave steepness s_{op}=0.035). Standard JONSWAP spectra were used. The number of waves was N=1000. Each structure was tested with four different water levels (WL), resulting in water depths at still water at the toe of the structure of d=0.089m, 0.119m, 0.149m and 0.179m (*i.e.* 0.03m increase in each case). Table 1 shows the mean values of the measured wave conditions at deep water and at the toe ($H_{1/3}$ denotes the significant wave height from the time-domain analysis and $T_{m-1,0}$ is the spectral wave period characterising effects of wave energy spectra on armour stability, wave run-up, wave overtopping, *etc*).

Table 1. Measured wave conditions at deep water and at the toe.

Water level		Deep		Toe				
Notation	d	H_{m0}	T_p	H_{m0}	$H_{1/3}$	$H_{2\%}$	T_m	$T_{m-1,0}$
	(m)	(m)	(s)	(m)	(m)	(m)	(s)	(s)
60%	0.089	0.088	1.27	0.039	0.030	0.035	1.21	1.59
80%	0.119	0.089	1.27	0.052	0.041	0.048	1.25	1.51
100%	0.149	0.089	1.27	0.065	0.052	0.061	1.23	1.41
120%	0.179	0.088	1.27	0.073	0.061	0.074	1.23	1.38

Six test series were performed, Series S1 and S2 with the structure in Figure 2, and Series S3 to S6 with one of the berm configurations in Figure 3. Except for Series S2, all series consisted of the four conditions mentioned in Table 1 without repair of the slope after each test, thus the resulting damage values are cumulative damage values. Series S1 with a uniform slope has been performed five times. In Series S2 only the 100% condition has been tested. This test was also performed five times. Damage to the rock armoured slope was measured using the Digital Stereo Photography technique (DSP) as described in Hofland *et al* (2011, 2014). With this measurement technique all displaced stones can be identified by comparing the images (*i.e.* a 3D digital representation of the slope) after a test run with the images of the initial slope, see Figure 4. Based on this technique all required parameters characterising damage can be determined.
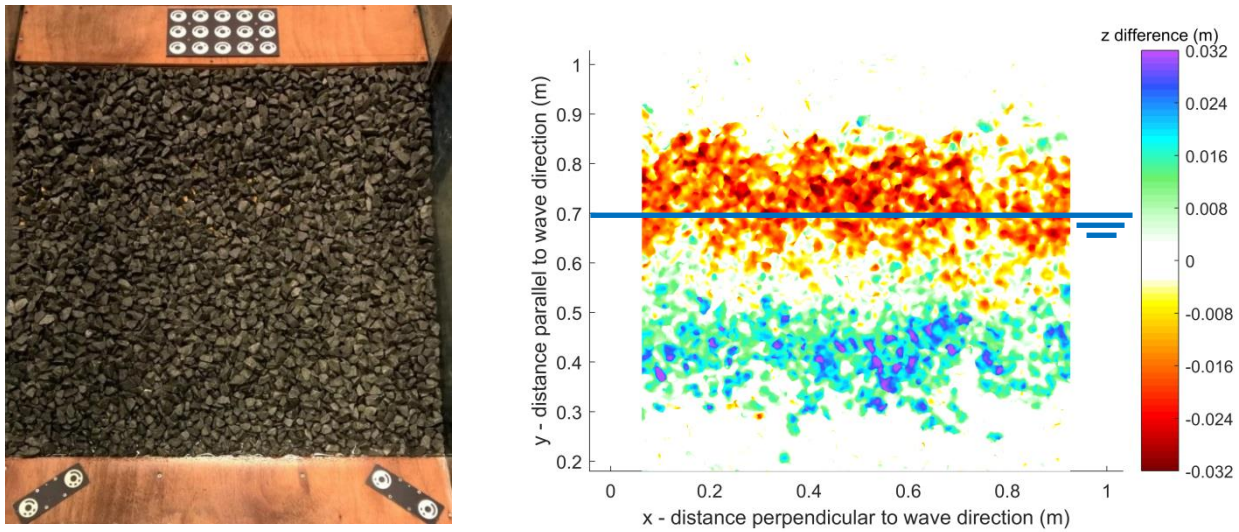

Figure 4. Image of the rock armoured slope (left) and an example of measurement (compared to the initial situation) of the distribution of damage using DSP, where the warm colours denote erosion and the cold colours denote accretion (right).

Figure 5 shows the non-dimensional erosion and deposition profiles for Series S1 and S2, averaged over five tests, including the 90% confidence intervals. On the horizontal axis y / D_{n50} denotes the intersection of the original profile of the armour and the still water level for the 100% condition. For all conditions erosion occurs around the still water level, with the maximum erosion depth slightly above the still water level.

The following parameters were used to characterise damage to the rock armoured slopes:

S = A_e / D_{n50}^2 where A_e is the eroded area comparing the profiles before the tests and after a test (Broderick, 1984); in the tests based on the average profile over the test section.

E_{2D} = d_e / D_{n50} where d_e is the maximum depth of erosion perpendicular to the slope (Melby and Kobayashi, 1998); in the tests based on the average profile over the test section.

$E_{3D,m}$ = d_e / D_{n50} where d_e is the maximum depth of erosion perpendicular to the slope, based on a moving average over a circular area of $m D_{n50}$ (Hofland *et al*, 2011, 2014).

Here, for the parameters S and E_{2D} the values averaged over a width of 0.88m (*i.e.* 54 stones with D_{n50} of 0.0163m) have been used. For the parameter $E_{3D,m}$ two values for m have been used m=1 and m=5.
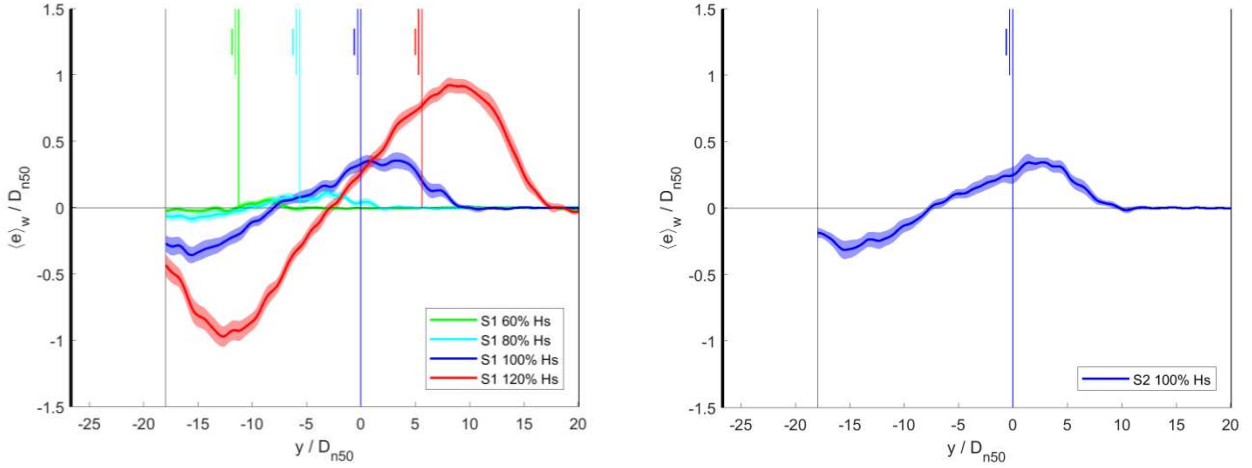
Figure 5. Non-dimensional erosion (positive values) and deposition (negative values) profiles averaged over 5 tests (Left: Series S1, for 4 different water levels; Right: Series S2 for the 100% water level), including 90%-confidence interval.

Table 2 shows the test results based on the width of the measurement section (*i.e.* 54 stones). Since the tests in Series S1 and Series S2 have been performed five times, the mean values (μ) and the standard deviations have been presented (σ). The tests with berm configurations (Series S3 to S6) have not been repeated (thus the numbers denote the actual test results; h_b denotes the water depth above the berm); the damage values are provided for the lower slope including the berm, and for the upper slope. The *S*-values for the entire slope are the summation of the two values. For the other damage parameters, the values for the entire slope are the maximum values of the two values (since the maximum damage occurs either at the lower slope or at the upper slope).

Table 2. Test results (μ denotes the mean value of the five tests and σ denotes the corresponding standard deviation; 'lower' denotes the slope below the berm plus the berm and 'upper' denotes the slope above the berm).

Series	Condition	Slope	S		E_{2D}		$E_{3D,1}$		$E_{3D,5}$	
			μ	σ	μ	σ	μ	σ	μ	σ
S1	60%	Uniform 1:3	0.3	0.044	0.07	0.027	1.07	0.050	0.17	0.016
	80%		0.9	0.278	0.16	0.024	1.15	0.096	0.35	0.044
	100%		3.7	0.413	0.41	0.044	1.45	0.077	0.73	0.093
	120%		11.4	0.445	0.96	0.086	2.13	0.220	1.31	0.120
S2	100%	Uniform 1:3	3.4	0.888	0.39	0.064	1.51	0.148	0.74	0.060

Series	Condition	Slope	S		E_{2D}		$E_{3D,1}$		$E_{3D,5}$	
			lower	upper	lower	upper	lower	upper	lower	upper
S3	60%	Wide berm B=0.16m, h_b=0.03m	0.1	0.0	0.03	0.00	1.13	0.12	0.18	0.01
	80%		1.1	0.0	0.15	0.01	1.11	0.25	0.28	0.02
	100%		1.7	0.3	0.25	0.08	1.35	1.15	0.44	0.20
	120%		1.5	1.0	0.25	0.16	1.35	1.15	0.38	0.38
S4	60%	Narrow berm B=0.08m, h_b=0.03m	0.4	0.0	0.07	0.01	0.93	0.15	0.15	0.03
	80%		0.8	0.0	0.13	0.01	1.07	0.72	0.32	0.08
	100%		2.8	0.1	0.51	0.03	1.40	0.95	0.81	0.18
	120%		2.9	1.9	0.58	0.31	1.40	1.32	0.86	0.53
S5	60%	Wide berm B=0.16m, h_b=0m	0.6	0.1	0.11	0.01	1.09	0.23	0.22	0.04
	80%		0.6	0.1	0.14	0.03	1.09	0.91	0.28	0.11
	100%		0.6	0.3	0.16	0.05	1.24	1.07	0.24	0.18
	120%		1.2	3.4	0.19	0.45	1.27	1.30	0.31	0.74
S6	60%	Narrow berm B=0.08m, h_b=0m	0.2	0.1	0.04	0.01	0.97	0.25	0.17	0.03
	80%		0.7	0.3	0.14	0.12	1.10	1.11	0.28	0.20
	100%		1.2	2.0	0.23	0.31	1.15	1.35	0.37	0.68
	120%		0.1	4.6	0.04	0.53	1.11	1.51	0.24	0.74

4

3   ANALYSIS OF RESULTS

The following observations can be made based on the tests results summarized in Table 2:

- Increasing water levels increase the wave loading and consequently the damage to the rock armour slopes. This increase in damage depends on the parameter to characterise damage. In the present tests the damage increased by a factor 44 for S, 15 for E_{2D}, 2 for $E_{3D,1}$ and 8 for $E_{3D,5}$.
- Comparing the damage values after the 100% condition in Series S1 (with 2 preceding conditions) with the 100% condition in Series S2 (without preceding conditions) indicate that the influence of the preceding conditions on the damage values (μ) is not statistically significant. The spreading (σ) in the damage is clearly larger for the one without preceding conditions, except for the last damage parameter ($E_{3D,5}$).
- The variations (σ / μ) in the test results for the damage parameters S and E_{2D} are relatively large for low damage values. The variations for these damage parameters are on average comparable but are larger than for the damage parameters $E_{3D,1}$ and $E_{3D,5}$. With the range of damage that is normally considered relevant $2 < S < 12$ (where $S = 2$ is characterised as start of damage and $S = 12$ as failure for the tested 1:3 slope), the variations in the damage values are comparable for the various damage parameters (S, E_{2D}, $E_{3D,1}$ and $E_{3D,5}$). However, for the tests without milder conditions prior to the design condition (*i.e.* 100% water level in Series S2) the variations in the damage parameters $E_{3D,1}$ and $E_{3D,5}$ are clearly less than for the damage parameters S and E_{2D}.
- For damage values larger than $S=1$, adding a berm leads to lower damage values than in the tests with a straight slope. For wider berms the effect of the berm increases (*i.e.* less damage). The structures with a submerged berm (h_b=0.03m) show less damage to the upper slope and more damage to the lower slope than the structures with the water level at the berm (h_b=0m). This is similar to results shown in Van Gent (2013).
- If damage is characterised by E_{2D} or $E_{3D,5}$ the berm is not always reducing the damage values, also not for the higher amounts of damage (*e.g.* 100% condition). The wide berms with a width of 10 stone diameters reduce the damage most effectively, irrespective of the damage parameter that is used.

As also discussed in Van Gent and Lim (2016), berms can be added to existing straight slopes to reduce overtopping and damage for increasing wave loading or water levels without increasing the crest level. Since the level of berms can be increased relatively easy once sea water levels increase, adding and/or modifying a berm can be seen as a useful measure for climate adaptation.

Figure 6 (left panel) shows the measured damage values S (based on the eroded area) versus and E_{2D} (based on the erosion depth). This figure shows a clear trend between these two parameters. The relevant range of damage is often between start of damage ($S=2$) and failure ($S=12$); within this range the trend can be simplified to $S = 10\ E_{2D}$ for the tested configurations (1:3 slopes, with and without a berm). Figure 6 (right panel) shows the measured damage values S (based on the eroded area) versus and $E_{3D,5}$. This figure also shows a clear trend between these two parameters. Within the relevant range of damage, this trend can be simplified to $S = 8\ E_{3D,5}^{2}$ for the tested configurations (1:3 slopes, with and without a berm).

The test results match reasonably well with existing empirical expressions for rock slope stability, with or without a berm. In De Almeida (2017) these comparisons are shown.
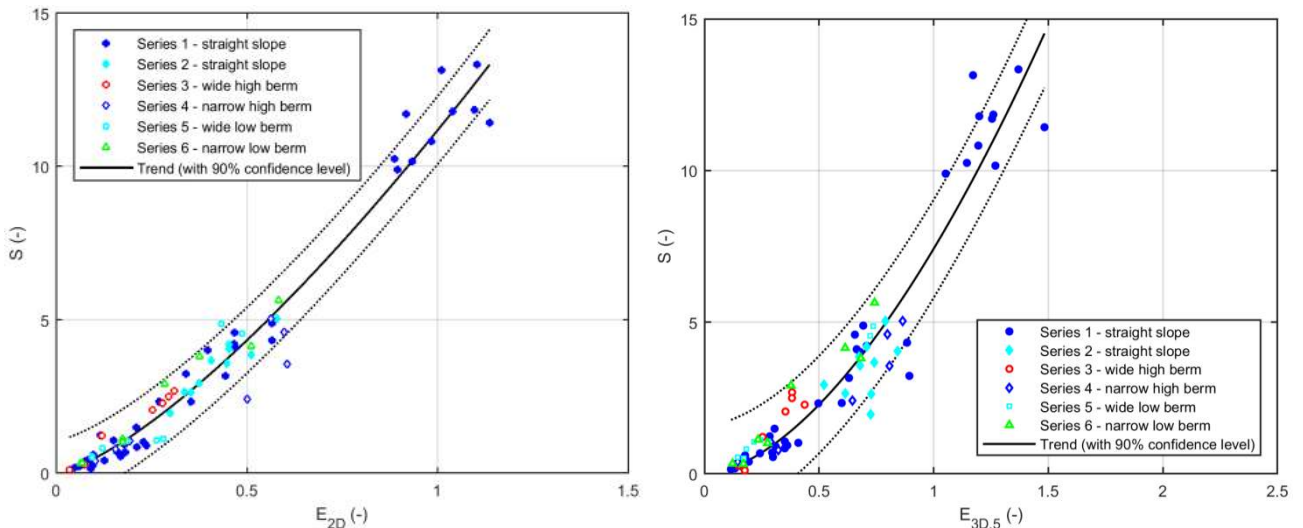

Figure 6. Left: Measured damage values S (based on the eroded area) versus and E_{2D} (based on the erosion depth); Right: damage values S (based on the eroded area) versus and $E_{3D,5}$ (characterisation width 27 stone diameters).

In the present tests the damage has been determined over a width that is equivalent to 54 stones of 0.0163m (*i.e.* somewhat less than the width of the flume due to the use of markers close to the glass walls of the flume for the Digital Stereo Photography technique). Series S1 was performed five times. Based on the results of Series S1, Figures 7, 8 and 9 show respectively the mean damage values, the standard deviations and the variations (*i.e.* the standard deviation σ

divided by the mean values μ) as function of the width over which the damage is determined [*i.e. S* (54) means that the mean and standard deviations of the damage are determined over a width of 54 stones (*i.e.* five observations, each from one of the five tests) and *S* (27) means that the mean and standard deviations of the damage are determined over a width of 27 stones (*i.e.* 10 observations, two from each of the five tests), *etc*]. These figures illustrate that damage values are affected by the width of which the damage is determined. This is not only valid for the present tests but for all physical model tests with rock slopes.

Figure 7 shows that the width over which the damage is obtained (*i.e.* the characterisation width) affects the values of the damage parameters. Figure 7a shows that for the damage parameter *S*, the mean values are more or less constant for a width of 10 stones or more. Figures 7c and 7d show that the mean values of the damage parameters $E_{3D,1}$ and $E_{3D,5}$ continue to increase for wider sections. This shows that the mean values of *S* (which is based on an average damage profile) become constant for a section (characterisation width) with a width of 10 stones or more while for the damage parameters $E_{3D,1}$ and $E_{3D,5}$ (which are maximal values in the section) the width of the section (in the tests and in reality) needs to be taken into account since the width determines the values and values continue to increase for wider sections.

a)   *S* parameter

b) E_{2D} parameter

c) $E_{3D,1}$ parameter
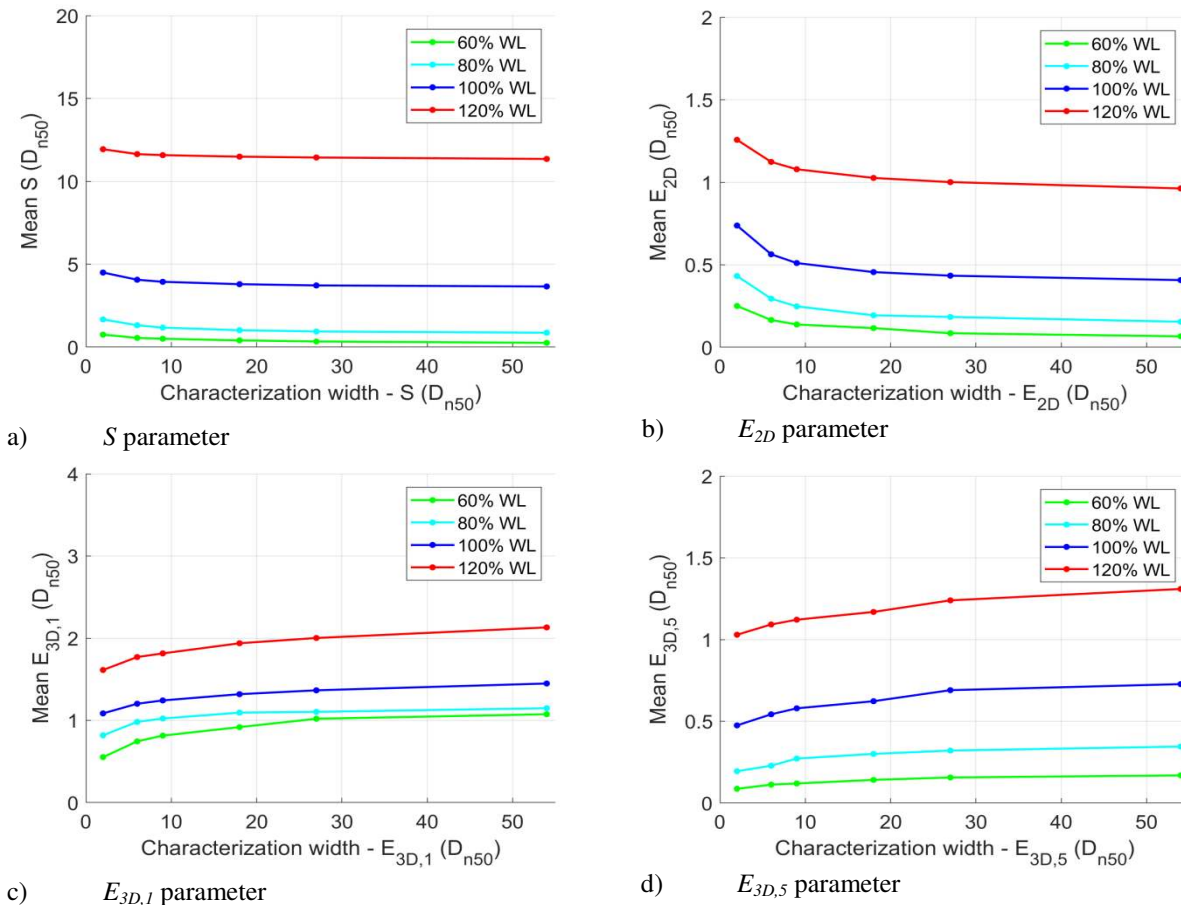
d) $E_{3D,5}$ parameter

Figure 7. Mean damage values versus characterisation width, *i.e.* the width over which the damage is determined (for Series S1); in each panel another damage parameter was used.

Figure 8 shows that the width over which the damage is obtained (*i.e.* the characterisation width) also affects the standard deviations of the damage parameters. Figure 8a shows that for the damage parameter *S*, the standard deviations are highly affected by the width of the section over which the damage is determined. Figure 8 shows that the standard deviations of the parameters E_{2D} and $E_{3D,5}$ are more or less constant for a section with a width of 25 stones or more.

Figure 9 shows the variation as function of the width over which the damage is obtained. For the lower damage values (*i.e.* at 60% and 80% water levels), the variability of the damage parameters $E_{3D,1}$ and $E_{3D,5}$ is less than for the damage parameters *S* and E_{2D}. For the higher damage values (*i.e.* at 100% and 120% water levels) and largest width of the test section (*e.g.* a width of 54 stones), there is no clear difference between the variation values of the various damage parameters. Figure 9 shows that the variation of the damage parameter $E_{3D,1}$ and $E_{3D,5}$ does not vary significantly for various widths over which the damage is obtained, as long as the width is about 25 stones or more. Note that for $E_{3D,1}$ and $E_{3D,5}$ the mean values increase for a larger width such that for equal values of the spreading the variations decrease for a larger width. As also discussed in De Almeida *et al* (2018), it is advised to determine the damage in a wave flume over a width of about 25 stones.

Besides that the width over which the damage is determined in the tests affects the damage values, there is also a difference between the width of the structure in the tests (scaled to prototype) and the width of the structure in reality. The present tests can be used to take this effect into account. This is the so-called length effect and this will be discussed in the following section.
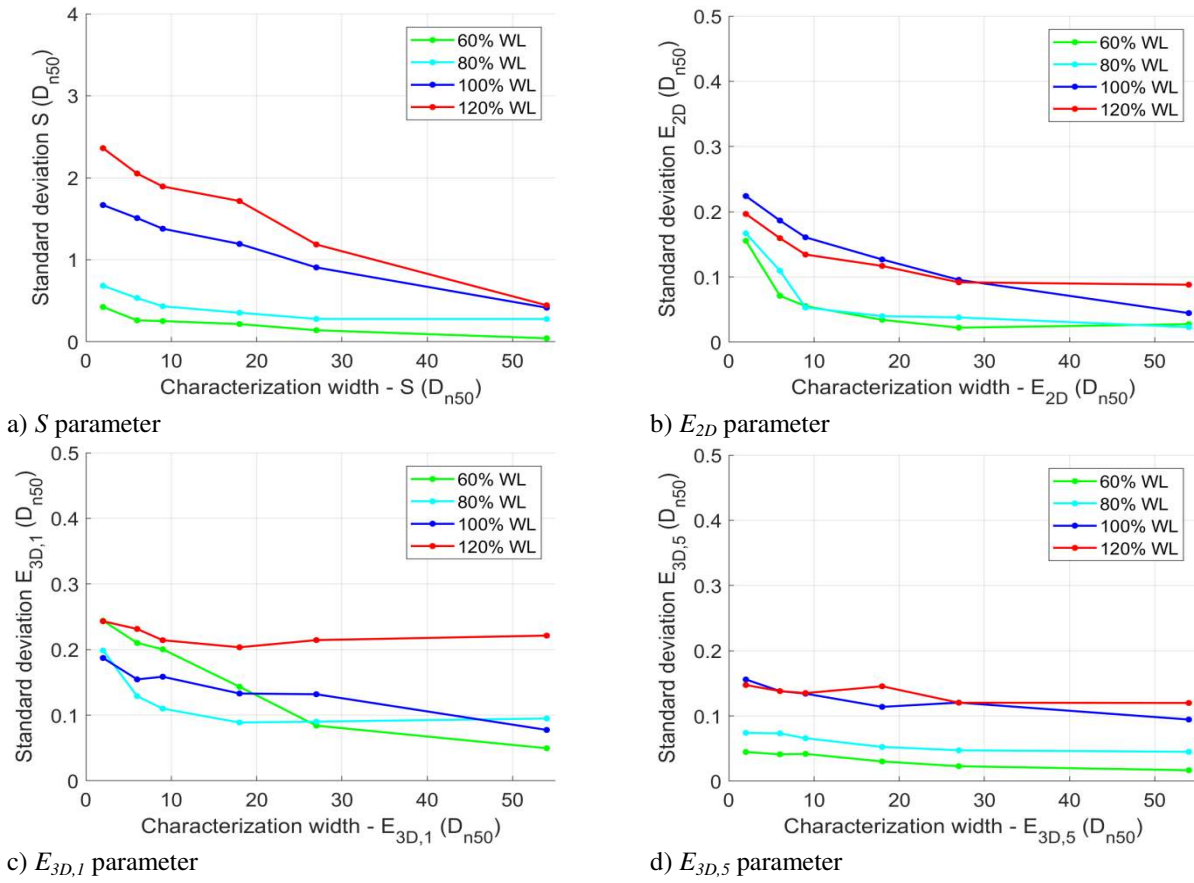
a) *S* parameter   b) *E_{2D}* parameter

c) *E_{3D,1}* parameter   d) *E_{3D,5}* parameter

Figure 8. Standard deviations of the damage values versus characterisation width, *i.e.* **the width over which the damage is determined (for Series S1).**

a) *S* parameter   b) *E_{2D}* parameter

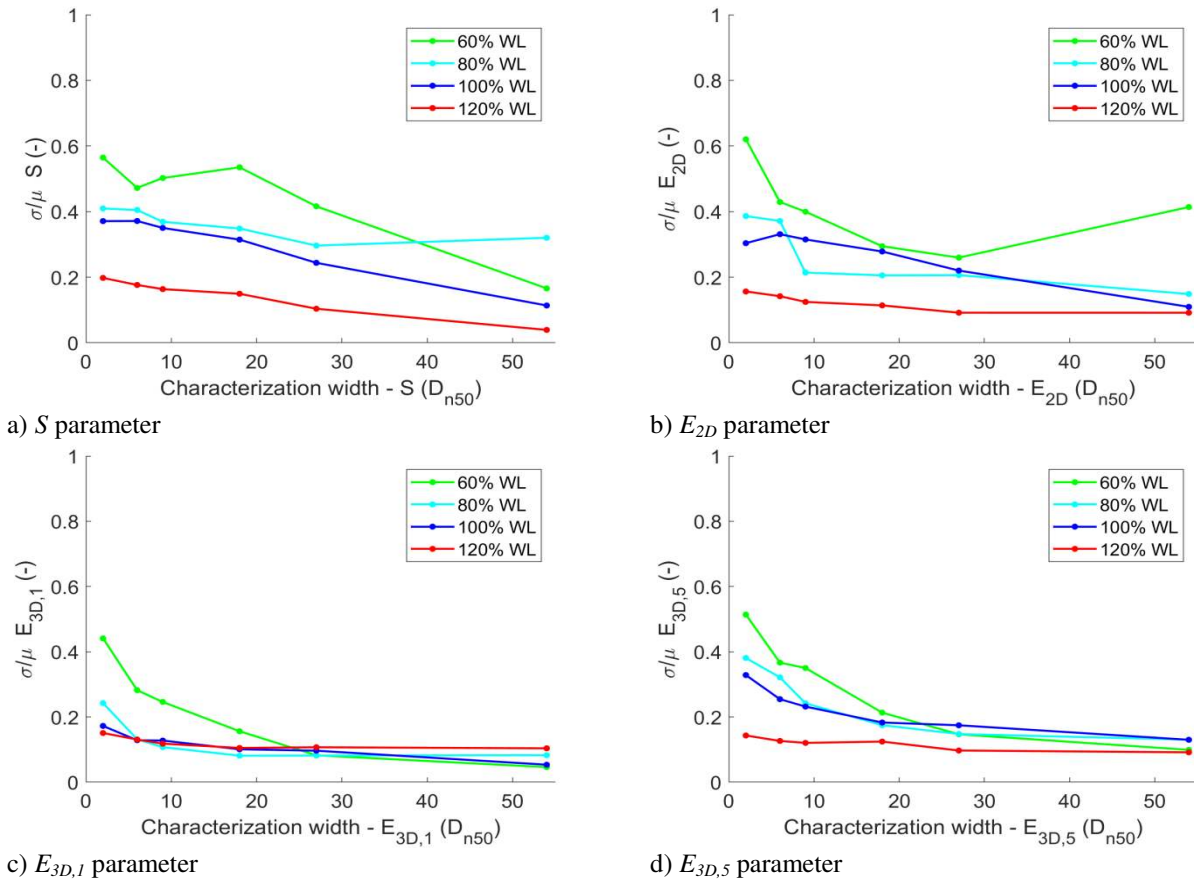c) *E_{3D,1}* parameter   d) *E_{3D,5}* parameter

Figure 9. Variation (*i.e.* **the standard deviation divided by the mean) in the damage versus characterisation width,** *i.e.* **the width over which the damage is determined (for Series S1).**

4   LENGTH EFFECT

Damage is normally measured over a specific width in a wave flume (here: 54 stones of 0.0163m). In reality the width of the structure is likely to be longer than the width (scaled to prototype dimensions) applied in the tests. Therefore, the mean and maximum damage in the real structure can deviate from the mean and maximum damage measured in the tests. This is called the length effect of the structure. In this section subscript m refers to model test results and subscript p refers to real (prototype) structures. Given that in this study tests have been repeated the mean values and standard deviations of the damage can be determined. These can be used to extrapolate the results in a narrow section (*i.e.* the test section) to a wider section, the width of the real structure. A number of assumptions are made in the following method of which the most important are that damage is normally distributed and that the spreading in the present tests is representative for other structures with rock slopes.

Due to the assumption that damage is normally distributed the probability that at any location within the test section the damage S is larger than the damage S_m obtained over the entire width of the measurement section is 50%, thus $P(S > S_m) = 0.5$. For practical situations in physical model tests this is considered as a reasonable assumption for damage numbers of $S_m \geq 2$. The probability that within this test section there is at any location damage that exceeds a pre-described critical damage S_{crit} (*i.e.* the maximum allowable damage) is denoted by $P(S > S_{crit})$.

$$P(S > S_{crit}) = 1 - F(S_m) \tag{1}$$

where $F(S_m)$ is the cumulative normal distribution, with the (mean) value S_m and standard deviation σ from the model tests [1].

To calculate the length effect due to the difference between the width of the test section, scaled to prototype scale L_m, and the width of the real structure L_p the ratio of these two $r = L_p / L_m$ is used. The probability that in the real (prototype) structure a critical damage is exceeded at any location is:

$$P(S_p > S_{crit}) = 1 - \left[F(S_m) \right]^r \tag{2}$$

where $F(S_m)$ is the same cumulative normal distribution, with the (mean) value S_m and the standard deviation σ from the model tests [1].

If a model test is performed without any repetitions, the standard deviation σ can be estimated based on the present tests. The standard deviation and variation (σ / μ, where $\mu = S_m$) appeared to be dependent on the amount of damage. The variation (σ / μ) reduces for larger damage values. For the damage parameter S, a simple fit can be used for applications between $2 < S < 12$: $\sigma = 0.3 S^{0.2}$. This relation is based on a characterisation width of 54 stones. Assuming that the standard deviations in the present tests are representative for all rock slopes, above mentioned expressions can be used for other physical models representing real structures using only the parameters r (for that particular structure), the measured damage S_m (for that particular test) and S_{crit} (for that particular structure in reality). This expression to relate the standard deviation to the amount of damage provides a robust estimation of the standard deviation. As can be seen in Table 2, the associated uncertainties in the estimates of the damage are large.

The width of the real (prototype) structure L_p can be divided into r sections with a (scaled) width of the test section L_m. The average damage profile in each of these r sections provides r values of S_p. Analogous to what is being assumed in the test section, the probability that at any location the damage S is larger than the damage value of that section S_p is 50%, thus $P(S > S_p) = 0.5$. The maximum damage of the r values of S_p will be higher than the damage in the model S_m. This maximum value (which is still a value based on an averaged profile over a width of L_m) can be calculated as follows:

$$S_p = F^{-1}\left(0.5^{\frac{1}{r}} \right) \tag{3}$$

where $F^{-1}(S)$ is the inverse of the cumulative normal distribution, with the value S_m and standard deviation σ, both from the model tests [2].

Above expressions can also be applied for the other mentioned damage parameters, but the expression to relate the standard deviation to the amount of damage varies per damage parameter:

$$S: \qquad \sigma = 0.3 S^{0.2} \tag{4a}$$

$$E_{2D}: \qquad \sigma = 0.9 E_{2D}^{0.7} \tag{4b}$$

---

[1] In Excel: $F(S_m)$ = NORM.DIST(S_{crit}; S_m; σ; TRUE)
[2] In Excel: S_p = NORM.S.INV(0.5^(1/r)) $\sigma + S_m$

$$E_{3D,1}: \qquad \sigma = 0.07\, E_{3D,1}^{1.5} \qquad\qquad\qquad\qquad\qquad (4c)$$

$$E_{3D,5}: \qquad \sigma = 0.1\, E_{3D,5} \qquad\qquad\qquad\qquad\qquad (4d)$$

These expressions lead to variations (σ / μ) that decrease for larger damage values using S or E_{2D}, increase for larger values using $E_{3D,1}$, and are constant for the damage parameter $E_{3D,5}$. Note that Melby and Kobayashi (1998) also derived estimates of the spreading depending on the amount of damage, but those are based on individual damage profiles and not on average damage profiles.

In above described expressions the assumption is made that the damage to the rock slope is normally distributed and consequently the maxima are Gumbel distributed. For all mentioned damage parameters (S, E_{2D}, $E_{3D,1}$ and $E_{3D,5}$) Eqs. 1 to 3 can be used. In contrast to the damage parameters S and E_{2D}, that are based on *average* damage profiles, the damage parameters $E_{3D,1}$ and $E_{3D,5}$ are based on *maximal* values that occurred over the width of the measurement section. Since the latter two are based on maxima, extreme value analysis can be used. To account for the difference between the width of the test section, scaled to prototype scale L_m, and the width of the real structure L_p the ratio of these two $r = L_p / L_m$ can be used to determine the damage value in the real structure, using the Gumbel distribution:

$$E_{3D} = \mu_G - \sigma_G\, \ln\left(-\ln\left(1 - \frac{1}{r}\right)\right) \qquad\qquad\qquad\qquad (5)$$

where μ_G and σ_G are the location and scale parameters of the Gumbel distribution which can be computed directly from the mean ($E_{3D,m}$) and standard deviation (σ) obtained from the model tests using $\sigma_G = \sigma\, 6^{0.5}/\ \pi$ and $\mu_G = E_{3D,m} - 0.577\,\sigma_G$.

To illustrate the importance of the length effect and taking into account spreading of the results, an example is given here based on Eq.1 to 5 (**bold** are assumed input values; in italic *red* the outcome of this example).

L	=	Width of the test section in the model:	**0.8m**
m	=	Model scale:	**50**
L_m	=	Width of the test section scaled to prototype scale (m):	40m
L_p	=	Width of the real (prototype) structure (m):	**1000m**
r	=	L_p / L_m	25
S_m	=	Damage observed a model test (based on the average profile):	**5**
σ	=	Standard deviation of the damage, using Eq.4a with $S = S_m = 5$:	0.414
S_p	=	Damage (maximum of r sections) in the real (prototype) structure, using Eq.3:	*5.80*
S_{crit}	=	Critical damage: Maximum allowable damage in the real (prototype) structure:	**6**
$P(S_m > S_{crit})$	=	Probability that S at any cross-section in a model is larger than S_{crit} (Eq.1):	*0.008*
$P(S_p > S_{crit})$	=	Probability that S at any cross-section in the real structure is larger than S_{crit} (Eq.2):	*0.179*

This example shows that for a model test with for instance a damage measured of $S=5$, there is a probability of 17.9% that in the real structure $S=6$ will be exceeded while the probability that $S=6$ will be exceeded in the tests is less than 1%. The damage value for the real structure (*i.e.* the maximum damage based on a damage profile averaged over a width of 40m in the real structure: the maximum value of 1000m/40m=25 damage values) will be higher than the damage in the model (*i.e.* the damage obtained based on the average profile in the measurement section): 5.80 versus 5.

In above described example the damage parameter S has been used, but the same can be done for the other three damage parameters, using the earlier mentioned expressions for the standard deviation σ per damage parameter.

$E_{3D,5\text{-}m}$	=	Damage observed a model:	**0.65**
σ	=	Standard deviation of the damage, using Eq.4d, with $E_{3D,5} = 0.65$:	0.065
$E_{3D,5\text{-}p}$	=	Damage in the real (prototype) structure, using Eq.3 (Normal distribution):	*0.775*
$E_{3D,5\text{-}p}$	=	Damage in the real (prototype) structure, using Eq.5 (Gumbel distribution):	*0.783*
$E_{3D\text{-}crit}$	=	Critical damage: Maximum allowable damage in the real (prototype) structure:	**0.8**
$P(E_{3D,5\text{-}m} > E_{3D\text{-}crit})$	=	Probability that $E_{3D,5}$ in a model is larger than $E_{3D\text{-}crit}$ (Eq.1):	*0.011*
$P(E_{3D,5\text{-}p} > E_{3D\text{-}crit})$	=	Probability that $E_{3D,5}$ in the real (prototype) structure is larger than $E_{3D\text{-}crit}$ (Eq.2):	*0.232*

This example shows that for a model test with for instance a damage measured of $E_{3D,5} = 0.65$, there is a probability of 23.2% that in the real structure $E_{3D,5} = 0.8$ will be exceeded. The damage in the real structure will be higher than the damage in the model; in case a normal distribution is used 0.775 versus 0.65 while in case the Gumbel distribution is used 0.783 versus 0.65. Thus, in this example the damage values for the real (prototype) structure are not sensitive to the applied approach.

In the approach described here, the measured spreading in Series S1 has been considered as representative, rather than Series S2. In Series S1 milder wave conditions were generated prior to the design condition (100% WL). This is considered as more representative for real structures since before reaching the peak of the storm (that is modelled in the model tests) also milder wave conditions occur earlier in a storm. In addition, it is likely that structures experience storms prior to the design storm. In Series S2 no milder conditions were present prior to the design condition. Therefore, the standard deviations in above-mentioned approach are based on Series S1 and not on Series S2. Note that, unlike the spreading, the mean damage values obtained in Series S1 and Series S2 are rather similar.

5   CONCLUSIONS AND RECOMMENDATIONS

Based on physical model tests the damage to rock armoured slopes was analysed for conditions with different water levels at still water. The wave conditions at deep water were the same but due to the shallow foreshore the wave conditions at the toe of the structure varied considerably. Tests with a straight slope and tests with berms were performed. Those with a straight slope were performed five times and this allowed for an analysis of the spreading in the tests results. The following conclusions can be drawn based on the described study:

- Increasing water levels can increase the damage to rock armour slopes considerably for structures with a shallow foreshore. In the performed tests the increasing water levels caused increasing wave loading and consequently an increase of the damage with a factor 2 (for $E_{3D,1}$) to 44 (for S) while the wave conditions at deep water were equal. Thus, this factor depends on which parameter is used to characterise damage.

- Wide berms (here with a width of 10 stone diameters) are effective to reduce the total damage to the armour layer, irrespective of the parameter that is used to characterise the damage. Berms can be added to existing straight slopes to reduce overtopping and damage for increasing water levels and increasing wave loading without increasing the crest level. Since the level of berms can be increased relatively easy once sea water levels increase, adding and/or modifying a berm can be seen as a useful measure for climate adaptation.

- The present tests can be used to estimate the spreading in the damage to rock armoured slopes for tests that have not been repeated so many times as in the present tests. Simple expressions have been derived to estimate the standard deviations and variations in damage to rock armoured slopes.

- With the range of damage that is normally considered relevant $2 < S < 12$ (where $S = 2$ is characterised as the start of damage and $S = 12$ as failure for the tested 1:3 slope), the variations in the damage values are comparable for the various damage parameters (S, E_{2D}, $E_{3D,1}$ and $E_{3D,5}$). However, for the tests without milder conditions prior to the design condition (i.e. 100% water level in Series S2) the variations in the damage parameters $E_{3D,1}$ and $E_{3D,5}$ are clearly less than for the damage parameters S and E_{2D}.

- If conditions with lower waves precede the design conditions the magnitude of the damage is similar to the situation where no conditions with milder waves precede the design condition. However, the variability in the damage increases if no conditions with milder waves precede the design condition.

- Since in 2D physical model tests structures are generally less wide than the real (prototype) structures that they resemble, the difference between the scaled width of the structure in the model and the width of the structure in reality needs to be taken into account. Expressions to take this length effect into account have been proposed.

Since the spreading in damage to rock armoured slopes is rather large, research is advised to study the spreading in damage to rock armoured slopes in more detail with even more repetitions than performed here. It is recommended to take the spreading in damage to rock armoured slopes into account in physical model tests and in reality; if only one test has been performed the presented tests can provide an estimate of the spreading. It is recommended to take the length effect into account if the structure in reality is wider than the scaled width of the model in a wave flume.

ACKNOWLEDGEMENTS

REFERENCES

Broderick, L. L., 1984. Riprap stability versus monochromatic and irregular waves, PhD thesis, Oregon State University.

De Almeida, E., 2017. Damage assessment of coastal structures in climate change adaptation, M.Sc.-report TU Delft, NL.

De Almeida, E., M.R.A. van Gent, B. Hofland, 2018. Damage characterisation of rock armoured slopes, Coastlab 2018.

Hofland, B., M. van Gent, T. Raaijmakers, F. Liefhebber, 2011. Damage evolution using the damage depth, Proc. Coastal Structures 2011, Yokohama.

Hofland, B., M. Disco, M.R.A. van Gent, 2014. Damage characterization of rubble mound roundheads, Coastlab 2014, Varna.

Melby, J. A. and N. Kobayashi, 1998. Progression and variability of damage on rubble mound breakwaters, Journal of Waterway, Port, Coastal, and Ocean Engineering 124(6), 286-294.

Van Gent, M.R.A., 2013. Rock stability of rubble mound breakwaters with a berm, Coastal Engineering, Elsevier, Vol. 78 p.35-45.

Van Gent, M.R.A. and L. Lim, 2016. Incorporating effects of oblique waves in the design of coastal protection structures under sea level rise, Sustainable Built Environment Conference (SBE16), September 2016, Singapore.